Hindawi
Advances in Civil Engineering
Volume 2018, Article ID 7923575, 11 pages
https://doi.org/10.1155/2018/7923575

Research Article

Axial Behaviour of Slender RC Circular Columns Strengthened with Circular CFST Jackets

Yiyan Lu[1], **Tao Zhu**[1], **Shan Li**[1], **Weijie Li**[1] **and Na Li**[2]

[1]*School of Civil Engineering, Wuhan University, Wuhan 430072, China*
[2]*School of Civil Engineering and Architecture, Wuhan University of Technology, Wuhan 430070, China*

Correspondence should be addressed to Shan Li; lishan@whu.edu.cn

Received 2 July 2018; Accepted 23 August 2018; Published 12 September 2018

Academic Editor: Eric Lui

This paper investigates the axial behavior of slender reinforced concrete (RC) columns strengthened with concrete filled steel tube (CFST) jacketing technique. It is realized by pouring self-compacting concrete (SCC) into the gap between inner original slender RC columns and outer steel tubes. Nine specimens were prepared and tested to failure under axial compression: a control specimen without strengthening and eight specimens with heights ranging between 1240 and 2140 mm strengthened with CFST jacketing. Experimental variables included four different length-to-diameter (L/D) ratios, three different diameter-to-thickness (D/t) ratios, and three different SCC strengths. The experimental results showed that the outer steel tube provided confinement to the SCC and original slender RC columns and thus effectively improved the behavior of slender RC columns. The failure mode of slender RC columns was changed from brittle failure (concrete peel-off) into ductile failure (global bending) after strengthening. And, the load-bearing capacity, material utilization, and ductility of slender RC columns were significantly enhanced. The strengthening effect of CFST jacketing decreased with the increase of L/D ratio and D/t ratio but showed little variation with higher SCC strength. An existing expression of load-bearing capacity for traditional CFST columns was extended to propose a formula for the load-bearing capacity of CFST jacketed columns, and the predictions showed good agreement with the experimental results.

1. Introduction

Strengthening of RC structures is critically important for several reasons [1–7]. One is to restore the load-bearing capacity of deteriorated concrete infrastructures because of aging or damage. Another reason is to enhance the serviceability and capacity of structures in response to a load demand increase beyond the original design. A third reason is to improve the load-bearing capacity for deficient members as a result of design or construction errors.

Common strengthening methods such as section enlargement (concrete jacketing) [8], externally bonded steel plates [9, 10], and externally bonded fiber-reinforced polymer (FRP) [11, 12] have been used for many years to improve structural service performance and ultimate capacity of concrete structures. However, their disadvantages may limit the further application. The concrete jacketing method obviously enlarges the cross section of concrete members, and the construction of steel cage and formwork costs a lot of labor and time. The steel plate strengthening hardly changes the appearance of concrete structures, but it requires a large amount of steel and antirust work [13–15]. The FRP strengthening degrades the deformation of concrete structures and the effective utilization of FRP typically ranges from 30 to 35% [16–19]. Therefore, new strengthening methods for concrete structures are still causing concern.

Recently, a novel technique, CFST jacketing, has become an option to strengthen concrete columns because of the superior performance of CFST columns (e.g., high load-bearing capacity and good ductility). It has been successfully applied in the strengthening of RC bridge piers [20, 21]. CFST jacketing is realized by the installation of in-field welded steel tube around the original RC column and

pouring concrete into the gap between the inner original column and outer steel tube. The CFST jacketing method has many preferable advantages. In addition to a significant increase of load-bearing capacity and ductility, the CFST jacketing method is quick and easy to apply because the outer steel tube could serve as formwork and steel reinforcement, and thus, it requires less temporary formwork and reduces the usage of steel. Moreover, it could better utilize properties of each material with little change in column section size.

To better understand the performance of RC structures strengthened with CFST jacketing, many studies have been conducted. Priestley et al. [22, 23] conducted experiments to verify the effectiveness of CFST jacketing approach for RC columns and concluded that the shear strength and ductility of RC columns were increased significantly. Sezen and Miller [24] compared the performances of bridge piers strengthened with FRP jacketing, concrete jacketing, and CFST jacketing. The results showed that the CFST jacketing method was much more effective in enhancing the load-bearing capacity and ductility. Wang [25] and He et al. [26] studied the effects of preloading on the compressive strength of CFST jacketed columns. The results showed that the preloading level had little effect on the load-bearing capacity of specimens. He et al. [27] also studied the axial compressive behavior of CFST jacketed columns with recycled aggregate concrete. The results showed that the influence of the recycled coarse aggregate replacement ratio on the compressive strength might be negligible. Recently, the authors of the present paper have also carried out experimental and theoretical studies on the axial and eccentric performance of CFST jacketed RC stub columns [28–30]. The influence of initial eccentricity on the strength of CFST jacketed RC column had been addressed.

Nevertheless, most of the previous studies are limited to stub columns, very limited research has been conducted to verify the effectiveness of CFST jacketing strengthening on slender RC columns. This paper presents an experimental study of slender RC columns strengthened with CFST jacketing under axial compression, and the SCC was used instead of normal concrete. The test program consists of nine specimens, one of which is unstrengthened and serves as control specimen, the remaining eight are strengthened with CFST jacketing. The main parameters in the test are the L/D ratio (5.7, 7.1, 8.4, and 9.8), D/t ratio (56.2, 67.4, and 121.7), and compressive strength of SCC (40, 50, and 60 MPa). A modified model is applied to predict the load-bearing capacity of strengthened slender RC columns.

2. Experimental Programme

2.1. Test Specimens. Nine columns were tested to failure under axial compression, including one control specimen (Ref) and eight CFST jacketed specimens which are named in the form of *tx-Cy-z*. The number after "*t*" represents the nominal thickness of steel tube. The number after "*C*" donates the design cubic compressive strength of SCC. The last number indicates the slenderness of columns. Table 1 summarizes the details of each specimen.

2.2. Preparation of Test Specimens. All original columns are circular with a diameter of 154 mm and variation of length (1240 mm, 1550 mm, 1850 mm, and 2140 mm). The reinforcement consists of 6 longitudinal steel rebars (12 mm diameter) and stirrups (6 mm diameter) spacing at 150 mm. The internal reinforcement ratio of the original column is 3.6% which meets the 0.6–5.0% range requirement [31]. The original columns are cast using C25-grade normal concrete and cured for 28 days in the laboratory. Afterward, the CFTS jacketing strengthening is followed.

(i) The original column is sandblasted by a hand grinder to remove the irregularities and debris

(ii) The outer steel tube is carefully placed on the designed region leaving a uniform gap

(iii) The SCC is poured into the gap between original columns and steel tube at three intervals

(iv) The strengthened column is then cured for 28 days in the laboratory

The reinforcement ratios of CFST jacketed columns range from 5.2% to 9.5%. The ratios are in the range of 3.0–20.0% which are commonly used by others' researches [32].

2.3. Material Properties. The original concrete and SCC are made from 42.5-grade Portland cement, aggregates with a maximum diameter of 20 mm, and river sand. Moreover, the water reducer, expansive agent, and fly ash are added to the SCC. The cubic compressive strength is determined with three $150 \times 150 \times 150$ mm concrete cubes after 28 days of cure. The mix design, cubic strength, and slump of concrete are summarized in Table 2.

The material properties of steel tubes, steel rebar, and stirrup are tested according to the Chinese code GB/T 50081-2002 [33]. The results are shown in Table 3.

2.4. Test Setup and Procedure. Eight strain gauges are bonded evenly on the exterior surface of the steel tube to measure the longitudinal and transverse strains at midheight. After the specimen is placed on the hinge supports, two linear variable differential transducers (LVDTs) are used to measure the axial shortening and three other LVDTs are placed to measure the lateral deflection along the specimen's height ($0.25\,L$, $0.50\,L$, and $0.75\,L$). The test is carried out with a universal hydraulic testing machine (capacity of 5000 kN). The load is applied in increments of one-tenth of the theoretical load-bearing capacity ($N_{u,theo}$) before the steel yield and in increments of one-fifteenth of $N_{u,theo}$ afterward. Each load interval is maintained for about 2 minutes as per Chinese code GB/T 50152-2012 [34]. The test setup and instrumentation are shown in Figure 1.

3. Experiment Results and Discussion

3.1. Failure Modes of Specimens. Specimen Ref exhibited a brittle failure. Concrete crack occurred near the top at 557 kN (about 85% of N_u). And the concrete cracks widened

Table 1: Specimen details.

Specimen	$D_2(D_1)\times t\times L$ (mm)	L/D_1	L/D_2	D_2/t	f_{cu1} (MPa)	f_{cu2} (MPa)	f_{sl} (MPa)	f_{s2} (MPa)	N_u (kN)	$N_{u,theo}$ (kN)	$N_{u,theo}/N_u$
Ref	154 × 0 × 1850	12.0	—	—	32.83	—	365	—	656	677	1.03
t3-C50-5.7	219 × 3.25 × 1240	8.1	5.7	67.4	32.83	52.58	365	352	2980	2622	0.88
t3-C50-7.1	219 × 3.25 × 1550	10.1	7.1	67.4	32.83	52.58	365	352	2810	2574	0.92
t3-C50-8.4	219 × 3.25 × 1850	12.0	8.4	67.4	32.83	52.58	365	352	2751	2525	0.92
t3-C50-9.8	219 × 3.25 × 2140	13.9	9.8	67.4	32.83	52.58	365	352	2703	2474	0.92
t2-C50-8.4	219 × 1.80 × 1850	12.0	8.4	121.7	32.83	52.58	365	390	2319	2621	1.13
t4-C50-8.4	219 × 3.90 × 1850	12.0	8.4	56.2	32.83	52.58	365	342	2932	2500	0.85
t3-C40-8.4	219 × 3.25 × 1850	12.0	8.4	67.4	32.83	43.01	365	352	2633	2373	0.90
t3-C60-8.4	219 × 3.25 × 1850	12.0	8.4	67.4	32.83	57.29	365	352	2845	2600	0.91

D_1 and D_2 are the diameters of unstrengthened and strengthened column; t is the measured thickness of outer steel tube; L is the length of column; f_{cu1} and f_{cu2} are the cubic compressive strengths of original concrete and SCC; f_{s1} and f_{s2} are the tensile strengths of steel rebar and steel tube; N_u and $N_{u,theo}$ are the experimental and theoretical load-bearing capacities of specimens.

Table 2: Mixes and properties of concrete.

Concrete	Cement	Sand	Gravel	Water	Water reducer	Expansive agent	Fly ash	Cubic strength (MPa)	Slump (mm)
RC C25	1.000	2.103	4.082	0.635	0.000	0.000	0.000	32.83	N/A
SCC C40	1.000	2.239	3.075	0.522	0.014	0.143	0.284	43.01	670
SCC C50	1.000	1.892	2.838	0.459	0.017	0.143	0.286	52.58	675
SCC C60	1.000	1.667	3.000	0.423	0.022	0.146	0.282	57.29	672

Table 3: Material properties of steel.

Steel	Diameter (mm)	Thickness (mm)	Young's modulus (GPa)	Yield strength (MPa)	Tensile strength (MPa)
Steel tube	219	1.80	191	390	587
Steel tube	219	3.25	211	352	425
Steel tube	219	3.90	234	342	522
Steel rebar	12	—	190	365	527
Stirrup	6	—	203	214	278

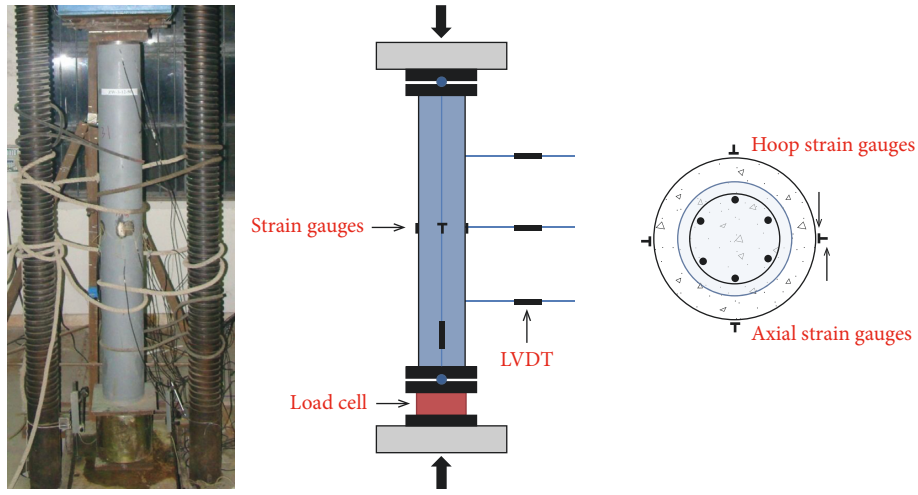

Figure 1: Test setup and instrumentation.

and propagated downwards with the increase of load. At the failure load (656 kN), the concrete on the top began to peel off without obvious axial shortening or lateral deflection, as shown in Figure 2(a). In comparison, all CFST jacketed columns failed in excessive lateral deflection, showing much better ductility. As the load increased, firstly the axial shortening and lateral deflection developed invisibly; secondly obvious axial shortening and lateral deflection were observed after the load reached around 85% of N_u; finally, excessive lateral deflection was obtained with the local buckling of outer steel tube at midheight, as shown in Figure 2(b). This observation is consistent with the research finding of traditional CFST columns [8, 35], where local buckling of steel tubes was also reported. It should be mentioned that our team has also conducted experiments of CFST jacketing strengthening on slender RC square columns

Figure 2: Typical failure modes of specimens. (a) Specimen Ref. (b) Specimen t3-C50-9.8.

[36]. After the specimens failed, the outer steel tubes were cut off and the crush of SCC at midheight was observed. When the SCC jackets were removed, obvious deflection of original columns and small cracks near the midheight were observed. It indicated that CFST jacketing could effectively change the failure mode of slender RC columns from brittle failure to ductile failure. And the failure at the similar location of each part (original column, SCC jacket, and outer steel tube) indicated they worked well together under the confine of outer CFST jackets.

3.2. Axial Load-Lateral Deflection Response. Figure 3 shows the typical curves of axial load and lateral deflection along height for CFST jacketed column. The curves along the height were basically a half-sine shape, and the biggest deflection was obtained at the midheight. The observable lateral deflection at N_u and unloading to 85% of N_u indicated good ductility of the specimen after CFST jacketing strengthening.

Figure 4 shows the axial load (N) versus the lateral deflection at midheight (Δ) response. The specimen Ref exhibited an almost linear curve, the load and midheight deflection at limit state were very low (656 kN and 0.47 mm), whereas the CFST jacketed columns exhibited an initial linear elastic phase before the load reached about 80% of N_u, followed by a curved ascending phase when outer steel tube began yielding and a smooth descending phase after N_u due to the buckling of columns. In general, all the CFST jacketed columns experienced an obvious lateral deflection at much higher load-bearing capacity. Figure 4(a) shows the influence of L/D ratio on the N-Δ response. The curves of specimens t3-C50-5.7, t3-C50-7.1, and t3-C50-8.4 had a similar linear phase but specimen t3-C50-9.8 behaved in

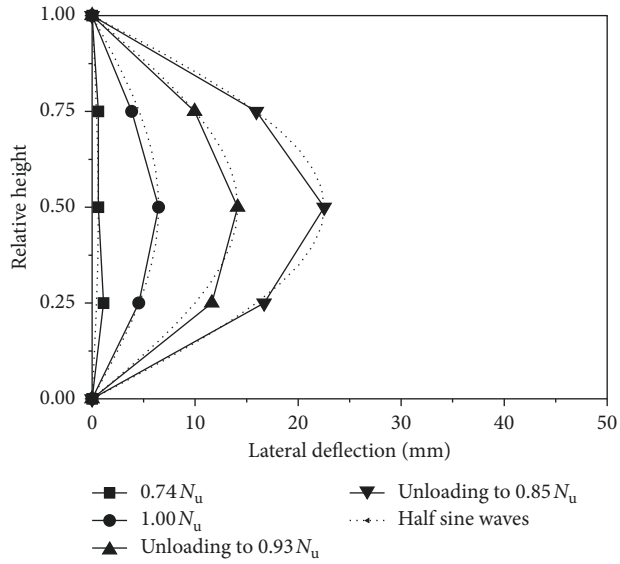

Figure 3: Typical load-lateral deflection curves (specimen t3-C50-8.4).

a softer manner with a larger deflection at the same load. It means that when the L/D ratio exceeds a certain value, the secondary moment could affect the behavior of CFST jacketed columns significantly. At the limit state, there was a lager deflection at a smaller ultimate strength when the L/D ratio increased from 5.7 to 9.8. Figure 4(b) shows the influence of D/t ratio on the N-Δ response. The specimen with thicker steel tube attained much higher ultimate strength. Figure 4(c) shows the influences of SCC strength on the N-Δ response. All the specimens exhibited similar curves. This is because that the flexural stiffness correlates with the elastic modulus of materials which varies slightly when the SCC

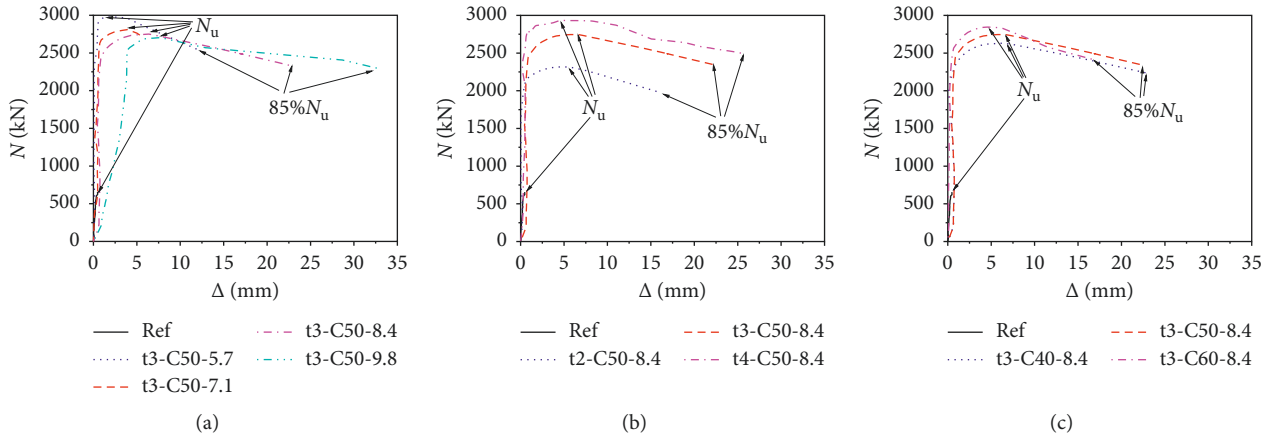

Figure 4: Axial load-lateral deflection response. (a) L/D ratio. (b) D/t ratio. (c) SCC strength.

strength increases from 40 to 60 MPa. However, a slight increase in ultimate strength was also observed.

3.3. Axial Load-Strain Response. Figure 5 shows the axial load (N) versus axial strain (ε_v) of outer steel tube response at midheight. The negative strain indicates compression and the positive strain indicates tension. Figure 5(a) shows the influence of L/D ratio on the development of axial strain during loading. In the initial loading stage, the maximum axial strain and the minimum axial strain of all the CFST jacketed columns were almost the same, indicating the axial strains were nearly uniform around the cross section. With the increase of the axial load, the L/D ratio affected the distribution of axial strain significantly. For specimens t3-C50-5.7 and t3-C50-7.1, the maximum axial strain grew much faster than the minimum axial strain when the load approached about 90% of N_u. While for specimens t3-C50-8.4 and t3-C50-9.8, this diversion happened at about 70% and 35% of N_u, and the minimum axial strain even changed from negative to positive. This nonuniform distribution of axial strain is because of the development of lateral deflection and the consequent secondary moment. Figure 5(b) shows the influence of D/t ratio on the N-ε_v response. After a linear increase of axial strain around the cross section, specimen t2-C50-8.4 experienced a curved ascending phase at about 1600 kN while specimens t3-C50-8.4 and t3-C50-8.4 kept increasing linearly up to about 2500 kN. Figure 5(c) shows the influence of SCC strength on the N-ε_v response. All the specimens exhibited similar curves with a slight variation of axial values at the limit state. The development of axial strain for specimens with different SCC strength almost overlapped during the loading, indicating that the SCC strength did not affect the behavior of the CFST columns significantly.

Figure 6 shows the relationship between the axial load (N) and hoop strain (ε_h) of outer steel tube at midheight in terms of L/D ratio, D/t ratio, and SCC strength. In general, the hoop strain near the compression side was much higher than that near the opposite side which even decreased to zero. This is because the dilation of SCC and original concrete was most active in the compression side and thus the most effective confinement was provided there. As shown in Figure 6(a), the maximum hoop strain of the outer steel tube showed a decreasing trend with the increase of L/D ratio, indicating a gradual decreasing confinement. As shown in Figure 6(b), specimen t2-C50-8.4 experienced a nonlinear increased hoop strain much earlier than specimens t3-C50-8.4 and t4-C50-8.4. As shown in Figure 6(c), specimens with different SCC strength exhibited similar curves, and only little differences were found after ultimate strength.

4. Discussion

4.1. Confinement. The outer steel tube confines the SCC and original concrete and thus increases their compressive strengths while the inner concrete suppresses the inward bulking of the outer steel tube.

This interaction enhances the load-bearing capacity, material utilization, and ductility of the CFST jacketed columns. The transverse deformation coefficient of the outer steel tube is adopted to evaluate the level of confinement and defined as $\varepsilon_h/\varepsilon_v$. Figure 7 shows the development of transverse deformation coefficient on the most compressive side ($\varepsilon_{hmax}/\varepsilon_{vmax}$) and the least-compressive side ($\varepsilon_{hmin}/\varepsilon_{vmin}$). In the initial loading stage (before 40% of N_u), the values of $\varepsilon_{hmax}/\varepsilon_{vmax}$ and $\varepsilon_{hmin}/\varepsilon_{vmin}$ ranged from 0.25 to 0.35, which were higher than that of concrete (usually 0.17–0.20). It indicated that the confinement was negligible in this stage because the dilation of inner concrete was smaller than that of the steel tube under the same axial deformation. When the axial load increased to 60–90% of N_u, the values of $\varepsilon_{hmax}/\varepsilon_{vmax}$ and $\varepsilon_{hmin}/\varepsilon_{vmin}$ for several specimens increased significantly beyond their initial values, indicating that the inner concrete was subjected to good confinement because the dilation was constrained by the outer steel tube. From Figure 7(a), the values of $\varepsilon_{hmax}/\varepsilon_{vmax}$ of specimens with L/D ratio from 5.7 to 9.8 were 0.91, 0.86, 0.64, and 0.66 while the values of $\varepsilon_{hmin}/\varepsilon_{vmin}$ were 0.44, 0.32, 0.28, and 0.49 at the ultimate limit state. This decreasing trend indicated the confinement was less effective with the increase of L/D ratio.

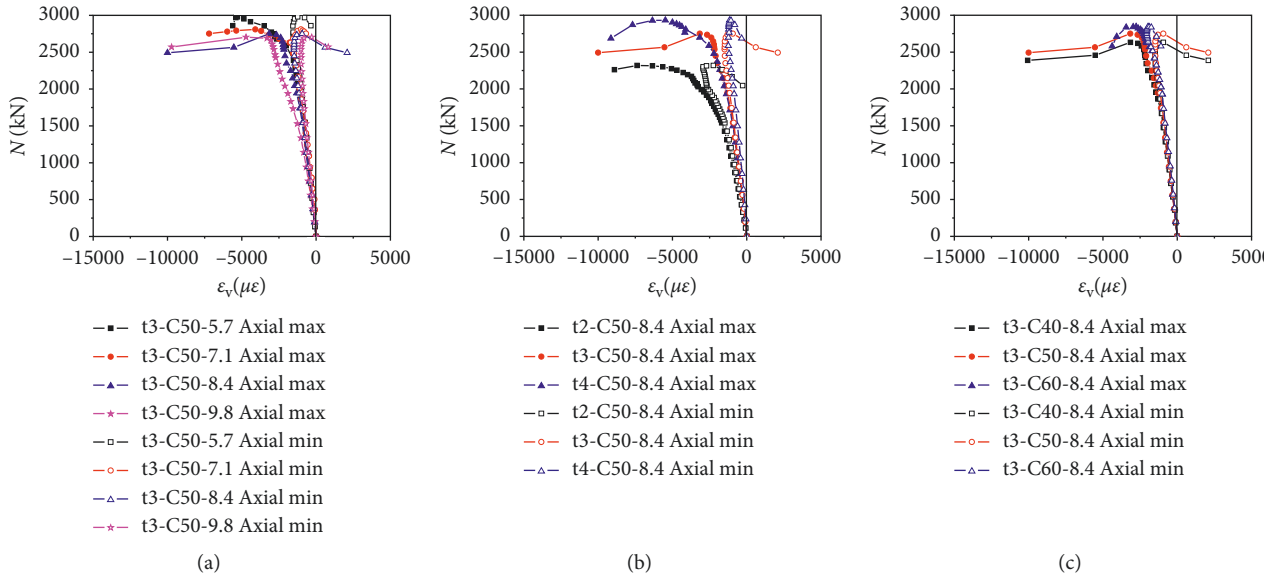

Figure 5: Axial load-axial strain of outer steel tube response. (a) L/D ratio. (b) D/t ratio. (c) SCC strength.

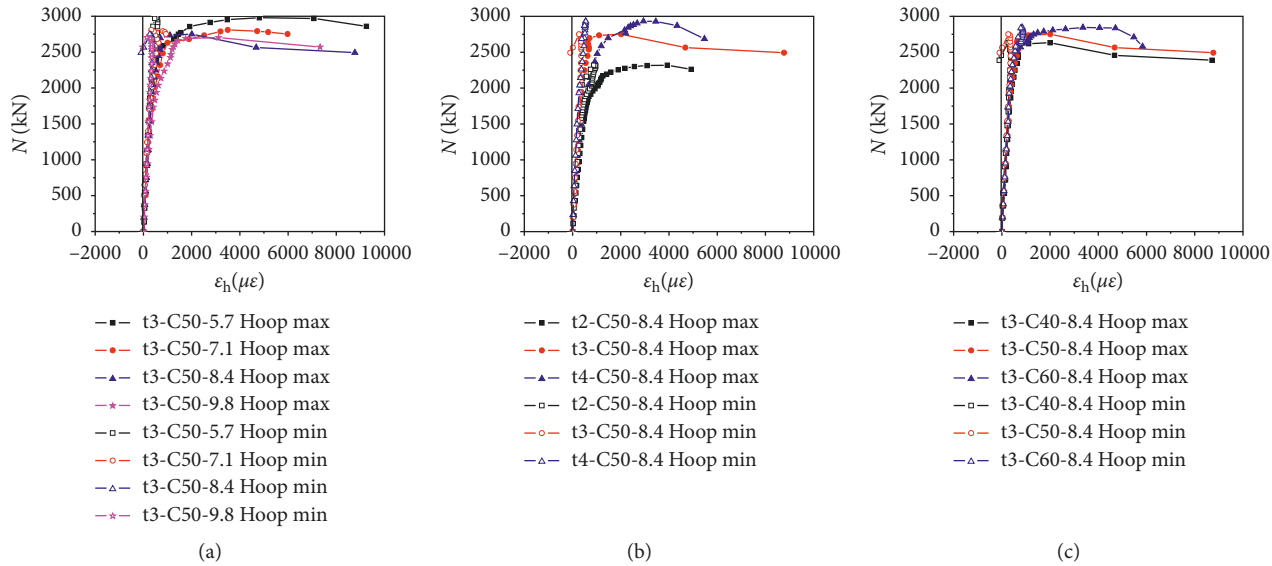

Figure 6: Axial load-hoop strain of outer steel tube response. (a) L/D ratio. (b) D/t ratio. (c) SCC strength.

It should be mentioned that although the value of $\varepsilon_{hmin}/\varepsilon_{vmin}$ of specimen t3-C50-9.8 was 0.49, it seemed that the confinement of the least-compressive side was more effective than other specimens. In fact, the value of $\varepsilon_{hmin}/\varepsilon_{vmin}$ for specimen t3-C50-9.8 was kept at 0.35 between 80 and 99.5% of N_u, indicating a negligible confinement. From Figure 7(b), on the most compressive side, the values of $\varepsilon_{hmax}/\varepsilon_{vmax}$ for specimens t2-C50-8.4, t3-C50-8.4, and t4-C50-8.4 were 0.53, 0.64 and 0.54 at N_u, indicating effective confinement. While on the least-compressive side, the values of $\varepsilon_{hmin}/\varepsilon_{vmin}$ were 0.39, 0.28, and 0.47. It means that the confinement was negligible for specimens t2-C50-8.4 and t3-C50-8.4, but the confinement was effective for specimen t4-C50-8.4. From Figure 7(c), the curves of specimens with different SCC strength agreed quite closely with each other except that stage after 85% of N_u, the $\varepsilon_{hmax}/\varepsilon_{vmax}$ and $\varepsilon_{hmin}/\varepsilon_{vmin}$ of specimen t3-C60-8.4 increased at a faster rate. It may be because that higher strength SCC is prone to forming splitting cracks and therefore, the circumferential stress in the steel tube increased rapidly.

4.2. Load-Bearing Capacity. The load-bearing capacities (N_u) of specimens are shown in Table 1 and compared in Figure 8 in terms of L/D ratio, D/t ratio, and SCC strength.

The N_u of t3-C50-8.4 was 2751 kN, which was 4.06 times $N_{u,theo}$ (calculated by equations in [31]) and 4.19 times N_u of specimen Ref. This significant enhancement indicated that the CFST jacketing method was effective to improve the load-bearing capacity of slender RC columns under axial

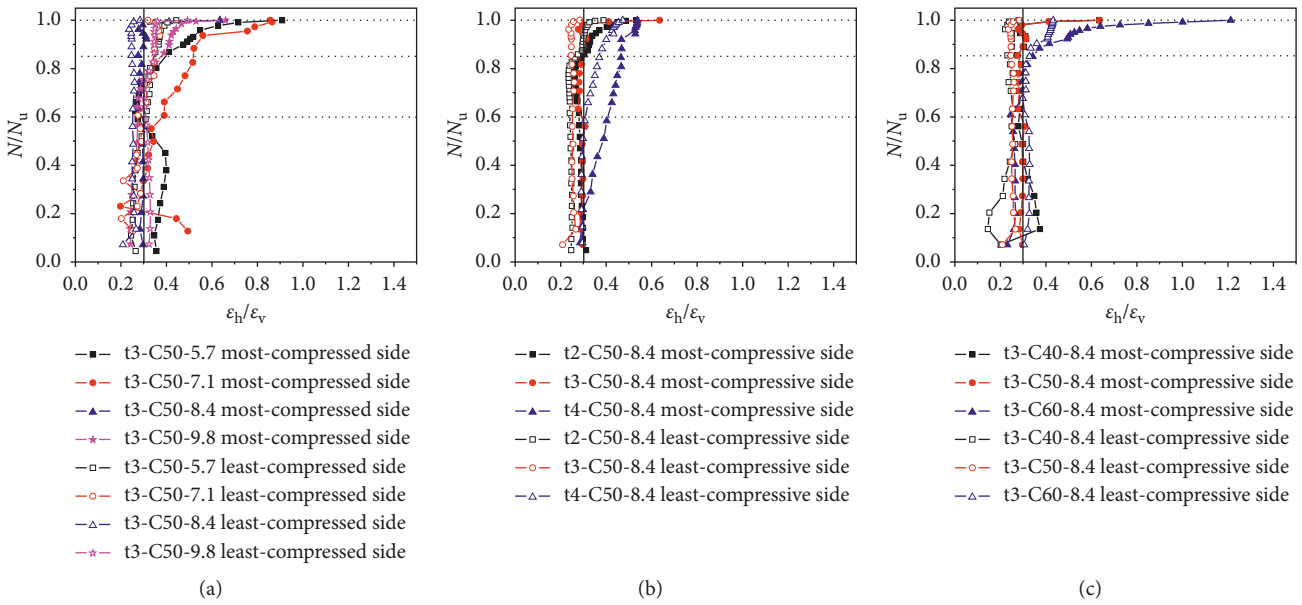

Figure 7: Normalised load-transverse deformation coefficient response. (a) L/D ratio. (b) D/t ratio. (c) SCC strength.

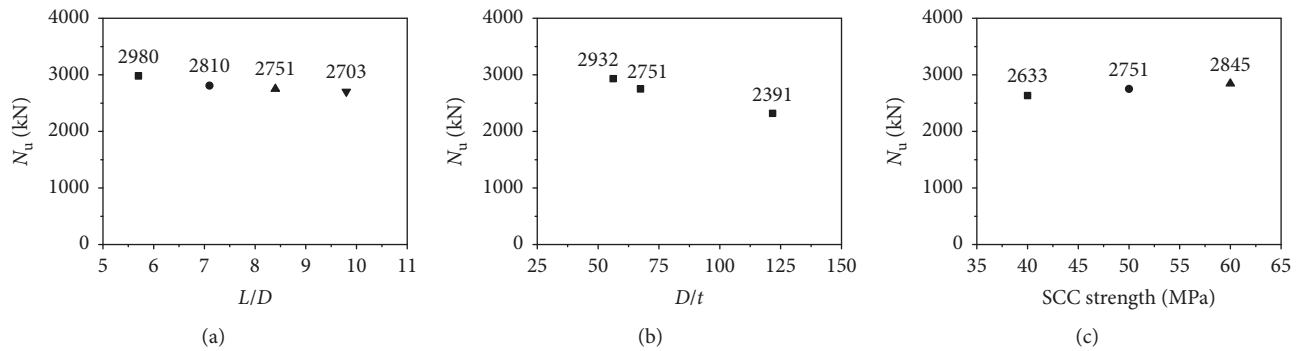

Figure 8: Load-bearing capacity of specimens. (a) L/D ratio. (b) D/t ratio. (c) SCC strength.

compression. On the other hand, the load-bearing capacity decreased progressively with larger L/D ratio. The N_u of specimens t3-C50-7.1, t3-C50-8.4, and t3-C50-9.8 were 5.7%, 7.7%, and 9.3% lower than that of specimen t3-C50-5.7, respectively. The load-bearing capacity decreased significantly with larger D/t ratio. It means that the load-bearing capacity decreased significantly with decreasing of steel CFST jacket thickness with the constant external diameter. The N_u of specimen t3-C50-8.4 and specimen t2-C50-8.4 were 6.2% and 20.9% lower than that of specimen t4-C50-8.4. The load-bearing capacity increased slightly with higher SCC strength. The N_u of specimen t3-C50-8.4 and specimen t3-C60-8.4 were 4.5% and 8.1% higher than that of specimen t3-C40-8.4. The load-bearing capacity increased with higher concrete strength as expected.

4.3. Strength Index. The utilization of the full plastic compressive resistance of a CFST column can be assessed through its strength index (SI) [8, 37]. Similarly, for CFST jacketed columns, SI is adopted to evaluate the effectiveness of material utilization and defined as

$$\mathrm{SI} = \frac{N_u}{f_{s1}A_{s1} + f_{s2}A_{s2} + f_{c1}A_{c1} + f_{c2}A_{c2}}, \quad (1)$$

where f_{c1} ($= 0.80 f_{cu1}$) and f_{c2} ($= 0.80 f_{cu2}$) are the compressive strengths of original concrete and SCC; A_{s1}, A_{s2}, A_{c1}, and A_{c2} are the cross-sectional areas of steel rebar, outer steel tube, original concrete, and SCC, respectively.

For specimen Ref, SI can also be calculated using Equation (1) when taking A_{s2} and A_{c2} as zero.

The SI of specimen Ref was only 0.89 while that of specimen t3-C50-8.4 was 1.24. It indicated that the slender RC column did not take full use of steel rebar and original concrete but the CFST jacketed column exhibited 124% utilization of materials. The 24% increase can be explained as follows:

(i) Under axial compression, the original concrete and SCC dilate laterally with the increase of load. However, the original concrete is confined by the

SCC jacket and the outer steel tube while the SCC is confined by the outer steel tube. It means that both the original concrete and SCC are under triaxial compression. The compressive strength of concrete under triaxial stress (f_{cc}) is higher than concrete compressive strength without confinement (f_c), and it can be written as [31]

$$f_{cc} = f_c + (4.5 \sim 7.0) f_L, \tag{2}$$

where f_L is the radial stress.

(ii) The existence of original concrete and SCC could avoid the inward local buckling of the outer steel tube and thus the material properties are better exploited.

This behavior of CFST jacketed columns also indicates that the significant increase in the load-bearing capacity is not only due to enlargement and additional steel reinforcement in cross section but also because of steel jacket's confinement.

Figure 9 compares the effects of L/D ratio, D/t ratio, and SCC strength on the SI of specimens. The SI decreased gradually with larger L/D ratio. The SI of specimens t3-C50-7.1, t3-C50-8.4, and t3-C50-9.8 were 5.2%, 7.5%, and 9.0% lower than that of t3-C50-5.7, respectively. The SI decreased significantly with larger D/t ratio. The SI of specimens t3-C50-8.4 and t2-C50-8.4 were 6.8% and 24.1% lower than that of t4-C50-8.4. But the SCC strength showed little influence on the SI of specimens. The SI of specimens t3-C50-8.4 and t3-C60-8.4 were only 1.6% and 0.8% lower than that of t3-C40-8.4.

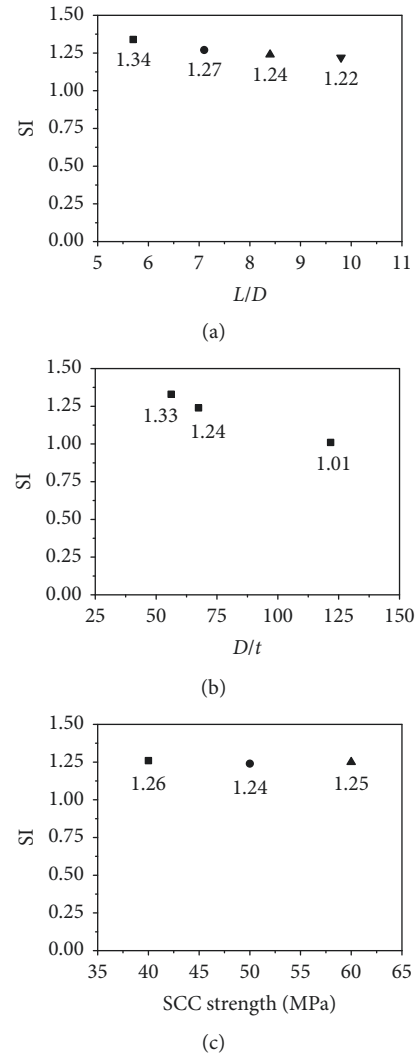

Figure 9: SI of specimens. (a) L/D ratio. (b) D/t ratio. (c) SCC strength.

4.4. Ductility. To qualify the ductility of a column, ductility index (DI) is often adopted by many researchers [8, 38]. Similarly, for CFST jacketed columns, DI is defined as

$$\mathrm{DI} = \frac{\Delta_{85\%}}{\Delta_u}, \tag{3}$$

where $\Delta_{85\%}$ is the midheight deflection when the load drops to 85% of the ultimate load on the unloading branch and Δ_u is the midheight deflection at the ultimate load.

The DI of specimen Ref was zero because there was no descending branch in the N-Δ curve while that of specimen t3-C50-8.4 was 3.48. It indicated that the CFST jacketing method was effective to improve the ductility of slender RC columns. Figure 10 shows the effects of L/D ratio, D/t ratio, and SCC strength on the DI of specimens. It should be mentioned that value of DI was not available for specimen t3-C50-7.1 due to the test having not been continued for sufficient deformation for the load to reduce to 85% of the ultimate load. Although there was fluctuation in the comparison of DI in terms of L/D ratio, the trend of decreasing DI with increasing slenderness might be clearly observed by linear fitting the experimental data. On the other hand, it was observed that there was a significant reduction in ductility with increasing D/t ratio and that the SCC strength did not have a large influence on the ductility of specimens. The DI of specimens t3-C50-8.4 and t2-C50-8.4 were 38.9% and 48.2% lower than that of t4-C50-8.4. The DI of specimens t3-C50-8.4 and t3-C60-8.4 were 1.8% and 4.4% higher than that of t3-C40-8.4.

4.5. Load-Bearing Capacity Prediction. Because the inner concrete and SCC worked well together under the confinement of outer steel tube, the CFST jacketed slender column failed similarly as the traditional CFST slender column.

Thus the load-bearing capacity prediction model for the traditional slender column may be also applied to CFST jacketed slender column when considering the different compressive strengths of original concrete and SCC and the contribution of longitudinal steel rebar. With reference to Chinese code GB 50936-2014 [39], a modified formula is proposed to predict the load-bearing capacity for CFST jacketed slender column:

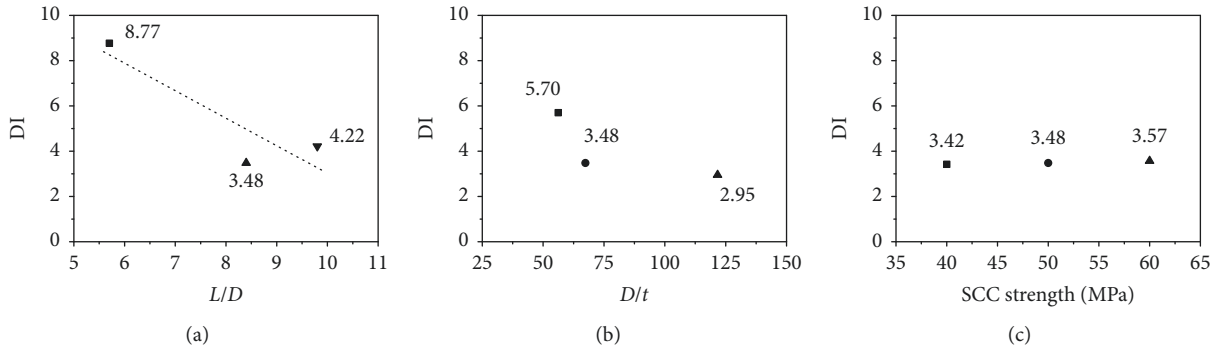

Figure 10: DI of specimens. (a) L/D ratio. (b) D/t ratio. (c) SCC strength.

$$N_{u,theo} = \varphi\left(f_{sc}A_{sc} + f_{s1}A_{s1}\right), \tag{4}$$

where φ is the slenderness reduction factor, f_{sc} is the compressive strength of CFST jacketed column, A_{sc} is the sum of the area of original concrete, SCC and outer steel tube.

f_{sc} can be written as

$$f_{sc} = \left[1.212 + \left(\frac{0.176f_{s2}}{213 + 0.974}\right)\xi + \left(\frac{-0.104f_c}{14.4 + 0.031}\right)\xi^2\right]f_c, \tag{5}$$

where ξ is the confinement index and f_c is the average concrete strength of original concrete and SCC, which are defined as

$$\xi = \frac{A_{s2}f_{s2}}{\left(A_{c1} + A_{c2}\right)f_c}, \qquad f_c = \frac{A_{c1}f_{c1} + A_{c2}f_{c2}}{A_{c1} + A_{c2}}. \tag{6}$$

φ can be calculated by a modified formula for traditional CFST slender column:

$$\varphi = \frac{1}{2\lambda_{sc1}^2}\left[\lambda_{sc1}^2 + \left(0.95 + 0.5\lambda_{sc1}\right) \cdot \sqrt{\left(\lambda_{sc1}^2 + \left(0.95 + 0.5\lambda_{sc1}\right)\right)^2 - 4\lambda_{sc1}^2}\right], \tag{7}$$

where λ_{sc1} is the regular slenderness ratio, which is defined as

$$\lambda_{sc1} = 0.01\lambda_{sc}\left(0.001f_{s2} + 0.781\right), \qquad \lambda_{sc} = \frac{\mu l}{i}, \qquad i = \sqrt{\frac{I_{sc}}{A_{sc}}} = \frac{D_2}{4}, \tag{8}$$

where λ_{sc} is the slenderness ratio and μl and i are the calculating length and radius of gyration of CFST jacketed column.

Table 1 compares the predicted strength ($N_{u,theo}$) with the experimental results (N_u) and the ratio $N_{u,theo}/N_u$ is 0.93 with a coefficient of variation (CV) of 0.09. The good agreement indicates the accuracy of the proposed model in predicting the load-bearing capacity for CFST jacketed slender column.

5. Conclusions

This paper presents an experiment of slender circular RC columns strengthened with CFST jacketing. Nine slender specimens were tested under axial compression, and the following conclusions can be drawn within the scope of this study:

(1) The CFST jacketed columns exhibited good ductile behavior under axial compression, and all experienced ductile failure mode (global bending), while the slender RC columns showed a brittle failure mode (concrete peel-off).

(2) The outer steel tube provided effective confinement on the SCC and original slender columns, and thus enhanced the load-bearing capacity, material utilization, and ductility of slender RC columns. The L/D ratio and D/t ratio showed obvious influence on the performance of CFST jacketed columns. The N_u, SI, and DI decreased 9.3%, 9.0%, and 51.9% when the L/D ratio increased from 5.7 to 9.8 and dropped 20.9%, 24.1%, and 48.2% when the D/t ratio increased from 56.2 to 121.7.

(3) The SCC strength had a slight effect on the performance of CFST jacketed columns, in which the specimen t3-C60-8.4 showed 8.1%, −0.8% and 4.4% increase in the N_u, SI, and DI compared to specimen t3-C40-8.4.

(4) A modified model was proposed to predict the load-bearing capacity for CFST jacketed slender columns based on the model for traditional CFST columns. Comparison between the prediction and the experimental results showed good agreement.

It is worth mentioning that the CFST jacketed column in practice may not behave similarly to specimens in this study because the external steel jacket may be discontinuous at the column top and bottom. For the CFST jacketed specimen under compression over the existing column and retrofit

area, the elastic stiffness increased more than 100% and strength increased up to 30% compared to the specimen compressed on the existing column only [24]. The structural steel collars were placed around the gaps at the top and bottom of the column and tied to the adjacent elements with postinstalled anchors aiming to increase shear strength locally [40]. The results showed this technique can transfer the column shears to the footing and adjacent elements and thus enhance the blast resistance to bridge columns seismically retrofitted using steel jackets. Therefore, the additional strengthening technique should be applied at the bottom and top of the column, such as structural steel collars, to transfer the whole axial load and shear force over the entire cross section. Otherwise, a relative reduction coefficient should be carefully considered before the application of CFST jacketing.

Conflicts of Interest

The authors declare that they have no conflicts of interest.

Acknowledgments

The authors are grateful for the financial supports provided by the Natural Science Foundation of China (51678456), the Fundamental Research Funds for the Central Universities of China (2015210020201), and the Hubei Provincial Natural Science Foundation of China (2016CFB271).

References

[1] S. T. Smith, S. J. Kim, and H. W. Zhang, "Behavior and effectiveness of FRP wrap in the confinement of large concrete cylinders," *Journal of Composites for Construction*, vol. 14, no. 5, pp. 572–582, 2010.

[2] G. F. Zhao, J. K. Xu, Y. L. Li, and M. Zhang, "Numerical analysis of the degradation characteristics of bearing capacity of a corroded reinforced concrete beam," *Advances in Civil Engineering*, vol. 2018, Article ID 2492350, 10 pages, 2018.

[3] Y. H. Guan, H. Q. Yuan, Z. Ge, Y. J. Huang, S. Li, and R. J. Sun, "Flexural properties of ECC-concrete composite beam," *Advances in Civil Engineering*, vol. 2018, Article ID 3138759, 7 pages, 2018.

[4] H. D. Yapa and J. M. Lees, "Rectangular reinforced concrete beams strengthened with CFRP Straps," *Journal of Composites for Construction*, vol. 18, no. 1, pp. 538–565, 2014.

[5] P. Kankeri and S. S. Prakash, "Experimental evaluation of bonded overlay and NSM GFRP bar strengthening on flexural behavior of precast prestressed hollow core slabs," *Engineering Structures*, vol. 120, pp. 49–57, 2016.

[6] T. Molkens, R. V. Coile, and T. Gernay, "Assessment of damage and residual load bearing capacity of a concrete slab after fire: applied reliability-based methodology," *Engineering Structures*, vol. 150, pp. 969–985, 2017.

[7] A. Abdullah and C. G. Bailey, "Punching behaviour of column-slab connection strengthened with non-prestressed or prestressed FRP plates," *Engineering Structures*, vol. 160, pp. 229–242, 2018.

[8] L. H. Han and Y. F. Yang, *Modern Concrete Filled Steel Tubular Structures*, China Architecture and Building Press, Beijing, China, 2004, in Chinese.

[9] S. Aykac, I. Kalkan, B. Aykac, S. Karahan, and S Kayar, "Strengthening and repair of reinforced concrete beams using external steel plates," *Journal of Structural Engineering*, vol. 139, no. 6, pp. 929–939, 2013.

[10] R. L. He, Y. Yang, and L. H. Sneed, "Seismic repair of reinforced concrete bridge columns: review of research findings," *Journal of Bridge Engineering*, vol. 20, no. 12, article 04015015, 2015.

[11] J. G. Dai, Y. L. Bai, and J. G. Teng, "Behavior and modeling of concrete confined with FRP composites of large deformability," *Journal of Composites for Construction*, vol. 15, no. 6, pp. 963–973, 2011.

[12] Z. Halabi, F. Ghrib, A. El-Ragaby, and K. Sennah, "Behavior of RC slab-column connections strengthened with external CFRP sheets and subjected to eccentric loading," *Journal of Composites for Construction*, vol. 17, no. 4, pp. 488–496, 2013.

[13] M. F. Petrou, D. Parler, K. A. Harries, and D. C. Rizos, "Strengthening of reinforced concrete bridge decks using carbon fiber-reinforced polymer composite materials," *Journal of Bridge Engineering*, vol. 13, no. 5, pp. 455–467, 2008.

[14] A. A. Elshafey, E. Rizk, H. Marzouk, and M. R. Haddara, "Prediction of punching shear strength of two-way slabs," *Engineering Structures*, vol. 33, no. 5, pp. 1742–1753, 2011.

[15] K. Qian and B. Li, "Strengthening and retrofitting of RC flat slabs to mitigate progressive collapse by externally bonded CFRP laminates," *Journal of Composites for Construction*, vol. 17, no. 4, pp. 554–565, 2013.

[16] R. Kotynia, R. Walendziak, I. Stoecklin, and U. Meier, "RC Slabs strengthened with prestressed and gradually anchored CFRP strips under monotonic and cyclic loading," *Journal of Composites for Construction*, vol. 15, no. 2, pp. 168–180, 2011.

[17] M. Staśkiewicz, R. Kotynia, and K. Lasek, "Flexural behavior of preloaded RC slabs strengthened with prestressed CFRP laminates," *Journal of Composites for Construction*, vol. 18, no. 3, pp. 318–320, 2014.

[18] J. M. Gallego, J. Michels, C. Czaderski, J. M. Gallego, J. Michels, and C. Czaderski, "Influence of the asphalt pavement on the short-term static strength and long-term behaviour of RC slabs strengthened with externally bonded CFRP strips," *Engineering Structures*, vol. 150, pp. 481–496, 2017.

[19] J. Alkhalil and T. El-Maaddawy, "Finite element modelling and testing of two-span concrete slab strips strengthened by externally-bonded composites and mechanical anchors," *Engineering Structures*, vol. 147, pp. 45–61, 2017.

[20] Y. H. Chai, "An analysis of the seismic characteristics of steel-jacketed circular bridge columns," *Earthquake Engineering and Structural Dynamics*, vol. 25, no. 2, pp. 149–1611, 2015.

[21] W. F. Chen and L. Duan, *Bridge Engineering Seismic Design*, China Machine Press, Beijing, China, 2008, in Chinese.

[22] M. J. N. Priestley, F. Seible, Y. Xiao, and R. Verma, "Steel jacket retrofitting of reinforced concrete bridge columns for enhanced shear strength: part 1—theoretical considerations and test design," *ACI Structural Journal*, vol. 91, no. 4, pp. 394–405, 1994.

[23] M. J. N. Priestley, F. Seible, Y. Xiao, and R. Verma, "Steel jacket retrofit for reinforced concrete bridge columns for enhanced shear strength—Part 2: test results and comparison with theory," *ACI Structural Journal*, vol. 91, no. 5, pp. 537–551, 1994.

[24] H. Sezen and E. A. Miller, "Experimental evaluation of axial behavior of strengthened circular reinforced-concrete columns," *Journal of Bridge Engineering*, vol. 16, no. 2, pp. 238–247, 2011.

[25] M. H. Wang, "Experimental study on axial-compression reinforced concrete column strengthened by circular steel tube," *Applied Mechanics and Materials*, vol. 94–96, pp. 1261–1270, 2011.

[26] A. He, J. Cai, Q. J. Chen, X. P. Liu, and J. Xu, "Behaviour of steel-jacket retrofitted RC columns with preload effects," *Thin-Walled Structures*, vol. 109, pp. 25–39, 2016.

[27] A. He, J. Cai, Q. J. Chen, X. P. Liu, H. Xue, and C. J. Yu, "Axial compressive behaviour of steel-jacket retrofitted RC columns with recycled aggregate concrete," *Construction and Building Materials*, vol. 141, pp. 501–516, 2017.

[28] Y. Y. Lu, H. J. Liang, S. Li, and N. Li, "Axial behavior of RC columns strengthened with SCC filled square steel tubes," *Steel and Composite Structures*, vol. 18, no. 3, pp. 623–639, 2015.

[29] Y. Y. Lu, H. J. Liang, S. Li, and N. Li, "Numerical and Experimental Investigation on Eccentric Loading Behavior of RC Columns Strengthened with SCC Filled Square Steel Tubes," *Advances in Structural Engineering*, vol. 18, no. 2, pp. 295–310, 2015.

[30] Y. Y. Lu, H. J. Liang, S. Li, and N. Li, "Eccentric strength and design of RC columns strengthened with SCC filled steel tubes," *Steel and Composite Structures*, vol. 18, no. 4, pp. 833–852, 2015.

[31] A. Q. Li, W. R. Cheng, and D. H. Yan, *Concrete Structure*, China Building Industry Press, Beijing, China, 2016, in Chinese.

[32] L. H. Han, *Concrete Filled Steel Tubular Structures*, Science Press, Beijing, China, 2007, in Chinese.

[33] GBT 50081-2010, *Standard for Test Method of Mechanical Properties on Ordinary Concrete. Ministry of Housing and Urban-Rural Development of the People's Republic of China (MOHURD)*, Architecture and Building Press, Beijing China, 2010, in Chinese.

[34] GB/T 50152-2012, *Standard for Test Method of Concrete Structures. Ministry of Housing and Urban-Rural Development of the People's Republic of China (MOHURD)*, China Building Industry Press, Beijing, China, 2012, in Chinese.

[35] B. Uy, Z. Tao, and L. H. Han, "Behaviour of short and slender concrete-filled stainless steel tubular columns," *Journal of Constructional Steel Research*, vol. 67, no. 3, pp. 360–378, 2011.

[36] J. F. Xue, *Research on compressive behavior of square rc column strengthened with self compacting concrete filled steel tube*, Ph. D. dissertation, Wuhan University, Wuhan, China, 2015, in Chinese.

[37] Y. Ye, S. J. Zhang, L. H. Han, and Y. Liu, "Square concrete-filled stainless steel/carbon steel bimetallic tubular stub columns under axial compression," *Journal of Constructional Steel Research*, vol. 146, pp. 49–62, 2018.

[38] Y. Y. Lu, N. Li, S. Li, and H. J. Liang, "Behavior of steel fiber reinforced concrete-filled steel tube columns under axial compression," *Construction and Building Materials*, vol. 95, pp. 74–85, 2015.

[39] GB 50936-201, *Technical Code for Concrete Filled Steel Tubular Structures. Ministry of Housing and Urban-Rural Development of the People's Republic of China (MOHURD)*, Architecture and Building Press, Beijing, China, 2014, in Chinese.

[40] P. Fouché, M. Bruneau, and V. P. Chiarito, "Modified Steel-jacketed columns for combined blast and seismic retrofit of existing bridge columns," *Journal of Bridge Engineering*, vol. 21, no. 7, article 04016035, 2016.